Meccanica (2005) 40: 181–202
DOI 10.1007/s11012-005-3306-4

Regular and Chaotic Vibrations of a Parametrically and Self-Excited System Under Internal Resonance Condition

JERZY WARMINSKI*
Department of Applied Mechanics, Lublin University of Technology, Nadbystrzycka 36, 20-618 Lublin, Poland

(Received: 23 March, 2004; accepted in revised form: 17 January, 2005)

Abstract. Vibrations of a parametrically and self-excited system with two degrees of freedom have been analysed in this paper. The system is constituted by two parametrically coupled oscillators characterised by self-excitation and nonlinear Duffing's type nonlinearities. Synchronisation phenomenon has been determined near the principal resonances in the neighbourhood of the first p_1 and the second p_2 natural frequencies, and near the combination resonance $(p_1 + p_2)/2$. Vibrations have been investigated for parameters which satisfy the internal resonance condition $p_2/p_1 = 3$. The existence and break down of the synchronisation phenomenon have been revealed analytically by the multiple time scale method, whilst transition of the system to chaotic motion has been carried out numerically.

Key words: Self-excitation, Parametric vibrations, Synchronisation, Internal resonance, Chaos.

1. Introduction

Interactions between vibrations originated by different sources can lead to very interesting phenomena [1,2]. Particularly, interactions between self- and parametrically excited vibrations produce quasi-periodic motion, but near some resonance regions, the synchronisation of the system frequency is observed, and then the system vibrates periodically. This phenomenon has been observed for one degree of freedom [3–5] and for two degrees models [6,7]. If the vibrating oscillator is additionally forced by a harmonic force, then inside the main parametric resonance, new solutions can appear [8,9]. The resonance curve possesses an internal loop. In such case, even five coexisting steady states of vibrations are possible. These kinds of phenomenon has been observed for one and two degrees of freedom systems [6,10]. Moreover, increase of parametric excitation transits the system from regular motion to chaos [5,7,11] or hyperchaos [10,12]. If the system is forced by energy source with limited power, then additional coupling in the system appears and new additional dynamic effects have been observed [10]. This kind of problem is called nonideal. Influence of nonideal energy source on the parametric and self-excited system has been presented by Warminski *et al*. [13] and Warminski [10,14]. Very often, papers devoted to many degrees of freedom systems concern the case when their natural frequencies are incommensurable numbers [6,10,12]. Dynamics of the parametrically and self-excited system can change radically if its natural frequencies ratio is a natural number [15,16]. Then, the

*e-mail: j.warminski@pollub.pl

system vibrates under the internal resonance condition. Due to the strong vibration modes interaction, the nature of motion can be different. In practical applications, for instance in manufacture dynamics [17], this kind of resonance is called 'mode coupling chatter'.

Interactions between parametrically and self-excited vibration under the internal resonance condition in the neighbourhood of synchronisation areas, is the main purpose of this paper. Besides, transition of the system to chaotic motion is pointed as well. As an example of practical engineering applications can be mentioned: vibrations of rotating shafts mounted in journal bearings and having different stiffness in two orthogonal directions [18], chatter vibrations in machining processes [19], gear boxes vibrations taking into account friction between teeth [20], cars' wheels vibrations due to radial changing stiffness and shimmy effect, or vibrations of an airplane's wing [4] or cables under flutter conditions [21–23]. The results of the paper may also be useful for control of nonlinear oscillations [24].

2. Model of the Vibrating System

A vibrating system (Figure 1) is composed of two masses coupled by a spring with stiffness changing periodically in time (parametric excitation of Mathieu's type). The model consists of a nonlinear Duffing's type spring and a nonlinear damper. The nonlinear damper described by the van der Pol's function $f_{d2}\left(x_2, x_2'\right) = \left(-c_2 - \hat{c}_2 x_2^2\right) x_2'$ is the source of the self-excitation of the system. Note that parameters having index 1 correspond to the first oscillator and index 2 to the second one, while mixed indexes mean coupling terms. Dynamics of the model is governed by the following two differential equations, expressed in generalised coordinates x_1 and x_2:

$$m_1 x_1'' + k_1 x_1 + \hat{k}_1 x_1^3 + \left(k_{12} - \hat{k}_{12}\cos 2\omega t\right)(x_1 - x_2) = 0, \tag{1}$$

$$m_2 x_2'' + f_{d2}(x, x') - \left(k_{12} - \hat{k}_{12}\cos 2\omega t\right)(x_1 - x_2) = 0. \tag{2}$$

Primes denote derivatives with respect to time. We introduce dimensionless time $\tau = \omega_1 t$, and coordinates $X_1 = x_1/x_0$, $X_2 = x_2/x_0$, where $\omega_1 = \sqrt{k_1/m_1}$ and $x_0 = m_1 g/k_1$ are the natural frequency and the static displacement of the first mass in case of

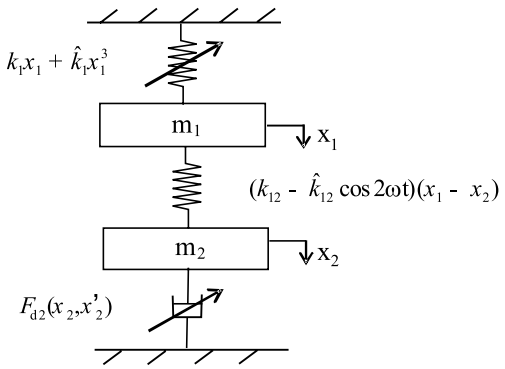

Figure 1. Physical model of the system.

absence of the coupling spring. Thus, differential equations of motions (1) and (2) take dimensionless forms:

$$\ddot{X}_1 + \delta_1 X_1 + \delta_{12}(X_1 - X_2) = \varepsilon\left[-\tilde{\gamma}_1 X_1^3 + \tilde{\mu}\cos 2\vartheta\tau(X_1 - X_2)\right], \tag{3}$$

$$\ddot{X}_2 - M\delta_{12}(X_1 - X_2) = \varepsilon M\left[-\tilde{F}_{d2}(X_2, \dot{X}_2) - \tilde{\mu}\cos 2\vartheta\tau(X_1 - X_2)\right]. \tag{4}$$

Dots indicate derivatives with respect to dimensionless time. A formal small parameter ε is also introduced in (3) and (4). To get the original set of parameters, it is necessary to multiply dimensionless parameters with 'tilde' by the formal small parameter i.e.

$$\alpha_2 = \varepsilon\tilde{\alpha}_2,\ \beta_2 = \varepsilon\tilde{\beta}_2,\ \gamma_1 = \varepsilon\tilde{\gamma}_1,\ \mu = \varepsilon\tilde{\mu},\ F_{d1} = \varepsilon\tilde{F}_{d1},\ F_{d2} = \varepsilon\tilde{F}_{d2},$$

where: $\vartheta = \omega/\omega_1$, $\delta_1 = 1$, $\delta_{12} = k_{12}/k_1$, $\mu = \hat{k}_{12}/k_1$, $M = m_1/m_2$, $\gamma_1 = x_0^2 \cdot \hat{k_1}/k_1$, are dimensionless coefficients. The function F_{d2} takes form: $F_{d2} = (-\alpha_2 + \beta_2 X_2^2)\dot{X}_2$,

where $\alpha_2 = c_2/(m_1\omega_1)$, $\beta_2 = x_0^2 \cdot \hat{c}_2/(m_1\omega_1)$.

For $\varepsilon = 0$, the system is linear and its natural frequencies are:

$$p_{1,2}^2 = \frac{1}{2}\left[(\delta_1 + \delta_{12}) + M\delta_{12} \mp \sqrt{(\delta_1 + \delta_{12} + M\delta_{12})^2 - 4M\delta_1\delta_{12}}\right]. \tag{5}$$

To solve the system analytically, the generalised coordinates X_1, X_2 have been transformed into quasi-normal co-ordinates Y_1 and Y_2:

$$Y_1 = \lambda_{11}X_1 + \lambda_{21}X_2, \qquad Y_2 = \lambda_{12}X_1 + \lambda_{22}X_2, \tag{6}$$

where

$$\lambda_{11} = 1,\ \ \lambda_{21} = \frac{\delta_1 + \delta_{12} - p_1^2}{\delta_{12}M},\ \ \lambda_{12} = 1,\ \ \lambda_{22} = \frac{\delta_1 + \delta_{12} - p_2^2}{\delta_{12}M}$$

are the corresponding vibrations modes. Substituting the quasi-normal co-ordinates into equations (3) and (4) we get

$$\ddot{Y}_1 + p_1^2 Y_1 = \varepsilon\left\{\tilde{F}_1(Y_1, Y_2, \dot{Y}_1, \dot{Y}_2, \tau) + M\lambda_{21}\tilde{F}_2(Y_1, Y_2, \dot{Y}_1, \dot{Y}_2, \tau)\right\}, \tag{7}$$

$$\ddot{Y}_2 + p_2^2 Y_2 = \varepsilon\left\{\tilde{F}_1(Y_1, Y_2, \dot{Y}_1, \dot{Y}_2, \tau) + M\lambda_{22}\tilde{F}_2(Y_1, Y_2, \dot{Y}_1, \dot{Y}_2, \tau)\right\}, \tag{8}$$

where

$$\tilde{F}_1(Y_1, Y_2, \dot{Y}_1, \dot{Y}_2, \tau) = -\tilde{\gamma}_1(Y_2\psi_1 - Y_1\psi_2)^3 + \tilde{\mu}\cos 2\vartheta\tau\,(Y_2\eta_1 - Y_1\eta_2),$$

$$\tilde{F}_2(Y_1, Y_2, \dot{Y}_1, \dot{Y}_2, \tau) = -\tilde{F}_{d2} - \tilde{\mu}\cos 2\vartheta\tau\,(Y_2\eta_1 - Y_1\eta_2)$$

and

$$\tilde{F}_{d2} = \left[-\tilde{\alpha}_2 + \tilde{\beta}_2\chi^2\,(Y_1 - Y_2)^2\right]\chi\left(\dot{Y}_1 - \dot{Y}_2\right)$$

is the nonlinear damping of the second oscillator. The parameters introduced in the coordinates transformation are defined as

$$\chi = \frac{1}{\lambda_{21} - \lambda_{22}}, \quad \psi_1 = \frac{\lambda_{21}}{\lambda_{21} - \lambda_{22}}, \quad \psi_2 = \frac{\lambda_{22}}{\lambda_{21} - \lambda_{22}}, \quad \eta_1 = \psi_1 + \chi, \quad \eta_2 = \psi_2 + \chi.$$

For $\varepsilon = 0$, equations (7) and (8) are uncoupled. However, in the considered case ε is assumed to be small and positive. It means that the system is weakly coupled. Moreover, we assume that internal resonance condition $p_2 = 3p_1$ is also satisfied. Due to cubic nonlinearity, we can expect that this kind of the internal resonance can play important role.

3. Analytical Solutions

3.1. Principal Parametric Resonance

Analytical solutions of the coupled nonlinear equations (7) and (8) can be determined by applying approximate methods. For weakly nonlinear system (small and positive value of ε) the multiple time scale method has been used [25]. Near the principal (the main) parametric resonances we can write:

- around the first natural frequency p_1

$$\vartheta^2 = p_1^2 + \varepsilon\sigma_1, \tag{9}$$

- around the second natural frequency p_2

$$\vartheta^2 = p_2^2 + \varepsilon\sigma_2, \tag{10}$$

where σ_1 and σ_2 are detuning parameters.

Around the first natural frequency we assume that the free frequencies relationship satisfies the internal resonance condition $p_2^2/p_1^2 = \nu_{21}^2$, where ν_{21} is a natural number. The last condition and equation (9) gives

$$\ddot{Y}_1 + \vartheta^2 Y_1 = \varepsilon\left\{\sigma_1 Y_1 + \tilde{F}_1(Y_1, Y_2, \dot{Y}_1, \dot{Y}_2, \tau) + M\lambda_{21}\tilde{F}_2(Y_1, Y_2, \dot{Y}_1, \dot{Y}_2, \tau)\right\}, \tag{11}$$

$$\ddot{Y}_2 + \nu_{21}^2\vartheta^2 Y_2 = \varepsilon\left\{\sigma_1\nu_{21}^2 Y_2 + \tilde{F}_1(Y_1, Y_2, \dot{Y}_1, \dot{Y}_2, \tau) + M\lambda_{22}\tilde{F}_2(Y_1, Y_2, \dot{Y}_1, \dot{Y}_2, \tau)\right\}. \tag{12}$$

We assume $\nu_{21} = 3$ considering a model characterised by the internal resonance condition $p_2/p_1 = 3$.

The approximate solution at the first-order of approximation is expressed in a power series of the small parameter ε:

$$Y_1(T_0, T_1, \varepsilon) = Y_{10}(T_0, T_1) + \varepsilon Y_{11}(T_0, T_1) + \cdots \tag{13}$$

$$Y_2(T_0, T_1, \varepsilon) = Y_{20}(T_0, T_1) + \varepsilon Y_{21}(T_0, T_1) + \cdots \tag{14}$$

and

$$T_n = \varepsilon^n \tau, \tag{15}$$

where $T_0 = \tau$, $T_1 = \varepsilon\tau$ are, respectively, the fast and slow time scales. According to Nayfeh [25], D_n^m means m order derivative with respect to n scale of time. After substituting the expansions (13) and (14) into (11), (12) we obtain equations at different perturbation orders

ε^0

$$D_0^2 Y_{10} + \vartheta^2 Y_{10} = 0, \tag{16}$$
$$D_0^2 Y_{20} + 9\vartheta^2 Y_{20} = 0, \tag{17}$$

ε^1

$$D_0^2 Y_{11} + \vartheta^2 Y_{11} = \sigma_1 Y_{10} - 2D_0 D_1 Y_{10} + \tilde{F}_{10} + M\lambda_{21}\tilde{F}_{20}, \tag{18}$$
$$D_0^2 Y_{21} + 9\vartheta^2 Y_{21} = 9\sigma_1 Y_{20} - 2D_0 D_1 Y_{20} + \tilde{F}_{10} + M\lambda_{22}\tilde{F}_{20}, \tag{19}$$

where

$$\tilde{F}_{10} = -\tilde{\gamma}_1 (\psi_1 Y_{20} - \psi_2 Y_{10})^3 + \tilde{\mu}\cos 2\vartheta\tau (\eta_1 Y_{20} - \eta_2 Y_{10}), \tag{20}$$
$$\tilde{F}_{20} = -\tilde{F}_{d20} - \tilde{\mu}\cos 2\vartheta\tau\, (\eta_1 Y_{20} - \eta_2 Y_{10}) \tag{21}$$

and

$$\tilde{F}_{d20} = \left[-\tilde{\alpha}_2 + \tilde{\beta}_2\chi^2 (Y_{20} - Y_{10})^2\right] \chi\, (D_0 Y_{20} - D_0 Y_{10})$$

describes van der Pol's damping at the first-order.

Under internal resonance condition, around the first natural frequency p_1 both, the first and the second natural modes can occur, therefore solutions of (16) and (17) are assumed as

$$Y_{10}(T_0, T_1, T_2) = A_{11}(T_1, T_2)\exp(i\vartheta T_0) + \bar{A}_{11}(T_1, T_2)\exp(-i\vartheta T_0), \tag{22}$$
$$Y_{20}(T_0, T_1, T_2) = A_{21}(T_1, T_2)\exp(3i\vartheta T_0) + \bar{A}_{21}(T_1, T_2)\exp(-3i\vartheta T_0), \tag{23}$$

where $i = \sqrt{-1}$ is the imaginary unit. The complex amplitudes $A_{11}(T_1, T_2)$, $A_{21}(T_1, T_2)$ are expressed in polar form:

$$A_{11}(T_1, T_2) = \frac{1}{2}a_1\exp(i\phi_1), \qquad A_{21}(T_1, T_2) = \frac{1}{2}a_2\exp(i\phi_2), \tag{24}$$

where a_1, a_2 and ϕ_1, ϕ_2 are, respectively, vibrations amplitudes and phases. After introducing the solutions (22), and (23) into (18), (19) the secular producing terms must be eliminated. Next separating real and imaginary parts we get the amplitudes and phases modulation equations (APMEs)

$$\begin{aligned} 2\vartheta\dot{a}_1 = {} & \frac{3}{4}\tilde{\gamma}_1 a_1^2 a_2 \psi_1 \psi_2^2 \sin(3\phi_1 - \phi_2) \\ & + \frac{1}{2}\tilde{\mu}\left[\eta_2 a_1 \sin 2\phi_1 - \eta_1 a_2 \sin(\phi_1 - \phi_2)\right](1 - M\lambda_{21}) \\ & + \left[-\tilde{F}_{d21} + \tilde{F}_{d22}\cos(3\phi_1 - \phi_2)\right] M\lambda_{21}, \end{aligned} \tag{25}$$

$$\begin{aligned} 2\varepsilon\vartheta a_1\dot{\phi}_1 = {} & a_1\left(p_1^2 - \vartheta^2\right) - \frac{3}{4}\varepsilon\tilde{\gamma}_1 a_1\psi_2\left(2a_2^2\psi_1^2 + a_1^2\psi_2^2\right) \\ & + \frac{1}{2}\varepsilon\tilde{\mu}\left[\eta_2 a_1\cos 2\phi_1 - \eta_1 a_2\cos(\phi_1 - \phi_2)\right](1 - M\lambda_{21}) \\ & + \frac{3}{4}\varepsilon\tilde{\gamma}_1 a_1^2 a_2\psi_1\psi_2^2\cos(3\phi_1 - \phi_2) - \varepsilon\tilde{F}_{d22}M\lambda_{21}\sin(3\phi_1 - \phi_2), \end{aligned} \tag{26}$$

$$2\vartheta\dot{a}_2 = \frac{1}{12}\tilde{\gamma}_1 a_1^3\psi_2^3\sin(3\phi_1-\phi_2) - \frac{1}{6}\tilde{\mu}\eta_2 a_1\sin(\phi_1-\phi_2)(1-M\lambda_{22}) + \left[\tilde{F}_{d23} - \tilde{F}_{d24}\cos(3\phi_1-\phi_2)\right]M\lambda_{22}, \tag{27}$$

$$2\varepsilon\vartheta a_2\dot{\phi}_2 = 3a_2\left(p_1^2-\vartheta^2\right) + \frac{1}{4}\varepsilon\tilde{\gamma}_1 a_2\psi_1\left(2a_1^2\psi_2^2 + a_2^2\psi_1^2\right) + \frac{1}{6}\varepsilon\tilde{\mu}\eta_2 a_1\left(1-M\lambda_{22}\right)\cos(\phi_1-\phi_2) - \varepsilon\tilde{F}_{d24}\sin\left(3\phi_1-\phi_2\right)M\lambda_{22} - \frac{1}{12}\varepsilon\tilde{\gamma}_1 a_1^3\psi_2^3\cos\left(3\phi_1-\phi_2\right). \tag{28}$$

Damping functions are defined as

$$\tilde{F}_{d21} = a_1\left(-\tilde{\alpha}_2 + \frac{1}{4}a_1^2\tilde{\beta}_2\chi^2 + \frac{1}{2}a_2^2\tilde{\beta}_2\chi^2\right)\vartheta\chi, \quad \tilde{F}_{d22} = \frac{1}{4}a_1^2 a_2\tilde{\beta}_2\vartheta\chi^3, \tag{29}$$

$$\tilde{F}_{d23} = a_2\left(-\tilde{\alpha}_2 + \frac{1}{4}a_2^2\tilde{\beta}_2\chi^2 + \frac{1}{2}a_1^2\tilde{\beta}_2\chi^2\right)\vartheta\chi, \quad \tilde{F}_{d24} = \frac{1}{12}a_1^3\tilde{\beta}_2\vartheta\chi^3. \tag{30}$$

Providing $\dot{a}_1 = 0$, $\dot{\phi}_1 = 0$, $\dot{a}_2 = 0$, $\dot{\phi}_2 = 0$, equations (25)–(28) allow us to find the amplitude and the phase of the steady–state vibrations. Particular solutions of (18) and (19) in connection with (22)–(24) give approximate solutions for the first and the second quasi-normal coordinate around natural frequency p_1

$$Y_1 = a_1\cos\left(\vartheta\tau + \phi_1\right) + \varepsilon\left(\ldots\right), \tag{31}$$

$$Y_2 = a_2\cos\left(3\vartheta\tau + \phi_2\right) + \varepsilon\left(\ldots\right). \tag{32}$$

Complete expressions for the approximate solutions are included in equations (A1) and (A2).

Around the second natural frequency the free frequencies relationship is expressed as $p_1^2/p_2^2 = \nu_{12}^2$ and then equations (7) and (8) get the form:

$$\ddot{Y}_1 + \nu_{12}^2\vartheta^2 Y_1 = \varepsilon\left\{\sigma_2\nu_{12}^2 Y_1 + \tilde{F}_1(Y_1, Y_2, \dot{Y}_1, \dot{Y}_2, \tau) + M\lambda_{21}\tilde{F}_2(Y_1, Y_2, \dot{Y}_1, \dot{Y}_2, \tau)\right\}, \tag{33}$$

$$\ddot{Y}_2 + \vartheta^2 Y_2 = \varepsilon\left\{\sigma_2 Y_2 + \tilde{F}_1(Y_1, Y_2, \dot{Y}_1, \dot{Y}_2, \tau) + M\lambda_{22}\tilde{F}_2(Y_1, Y_2, \dot{Y}_1, \dot{Y}_2, \tau)\right\}. \tag{34}$$

Now, (34) is a leading equation and $\nu_{12} = 1/3$. Substitution of the expansions (13), (14) in (33), (34) gives

ε^0

$$D_0^2 Y_{10} + \frac{1}{9}\vartheta^2 Y_{10} = 0, \tag{35}$$

$$D_0^2 Y_{20} + \vartheta^2 Y_{20} = 0, \tag{36}$$

ε^1

$$D_0^2 Y_{11} + \frac{1}{9}\vartheta^2 Y_{11} = \frac{1}{9}\sigma_2 Y_{10} - 2D_0 D_1 Y_{10} + \tilde{F}_{10} + M\lambda_{21}\tilde{F}_{20}, \tag{37}$$

$$D_0^2 Y_{21} + \vartheta^2 Y_{21} = \sigma_2 Y_{20} - 2D_0 D_1 Y_{20} + \tilde{F}_{10} + M\lambda_{22}\tilde{F}_{20}, \tag{38}$$

where $\tilde{F}_{10}$ and $\tilde{F}_{20}$ are defined by (20) and (21). Solutions for the first and the second natural modes get forms:

$$Y_{10}(T_0, T_1, T_2) = A_{11}(T_1, T_2)\exp\left(\frac{1}{3}i\vartheta T_0\right) + \bar{A}_{11}(T_1, T_2)\exp\left(-\frac{1}{3}i\vartheta T_0\right), \tag{39}$$

$$Y_{20}(T_0, T_1, T_2) = A_{21}(T_1, T_2)\exp(i\vartheta T_0) + \bar{A}_{21}(T_1, T_2)\exp(-i\vartheta T_0). \tag{40}$$

Substituting equations (39) and (40) into (37), (38) and eliminating the secular producing terms we get modulation equations:

$$2\vartheta\dot{a}_1 = \frac{9}{4}\tilde{\gamma}_1 a_1^2 a_2 \psi_1 \psi_2^2 \sin(3\phi_1 - \phi_2) + \left[-\tilde{F}_{d21} + \tilde{F}_{d22}\cos(3\phi_1 - \phi_2)\right] M\lambda_{21}, \tag{41}$$

$$\begin{aligned} 2\varepsilon\vartheta a_1\dot{\phi}_1 = {} & \frac{1}{3}a_1\left(p_2^2 - \vartheta^2\right) - \frac{9}{4}\varepsilon\tilde{\gamma}_1 a_1\psi_2\left(2a_2^2\psi_1^2 + a_1^2\psi_2^2\right) \\ & + \frac{9}{4}\varepsilon\tilde{\gamma}_1 a_1^2 a_2\psi_1\psi_2^2\cos(3\phi_1 - \phi_2) - \tilde{F}_{d22}M\lambda_{21}\sin(3\phi_1 - \phi_2), \end{aligned} \tag{42}$$

$$\begin{aligned} 2\vartheta\dot{a}_2 = {} & \frac{1}{4}\tilde{\gamma}_1 a_1^3\psi_2^3\sin(3\phi_1 - \phi_2) - \frac{1}{2}\tilde{\mu}\eta_1 a_2(1 - M\lambda_{22})\sin 2\phi_2 \\ & + \left[\tilde{F}_{d23} - \tilde{F}_{d24}\cos(3\phi_1 - \phi_2)\right] M\lambda_{22}, \end{aligned} \tag{43}$$

$$\begin{aligned} 2\vartheta a_2\varepsilon\dot{\phi}_2 = {} & a_2\left(p_2^2 - \vartheta^2\right) + \frac{3}{4}\varepsilon\tilde{\gamma}_1\psi_1 a_2\left(2a_1^2\psi_2^2 + a_2^2\psi_1^2\right) \\ & - \frac{1}{4}\varepsilon\tilde{\gamma}_1 a_1^3\psi_2^3\cos(3\phi_1 - \phi_2) - \frac{1}{2}\varepsilon\tilde{\mu}\eta_1 a_2(1 - M\lambda_{22})\cos 2\phi_2 \\ & - \tilde{F}_{d24}M\lambda_{22}\sin(3\phi_1 - \phi_2). \end{aligned} \tag{44}$$

Around the second natural frequency p_2 the steady-state approximate solutions are:

$$Y_1 = a_1\cos\left(\frac{1}{3}\vartheta\tau + \phi_1\right) + \varepsilon(\ldots), \tag{45}$$

$$Y_2 = a_2\cos(\vartheta\tau + \phi_2) + \varepsilon(\ldots). \tag{46}$$

Full expressions for the approximate solutions are included in equations (A3) and (A4). Analysis of (41)–(44) show that in a steady state $\dot{a}_1 = 0$, $\dot{\phi}_1 = 0$, $\dot{a}_2 = 0$, $\dot{\phi}_2 = 0$, around the second natural frequency p_2, two types of solutions are possible

- nontrivial solution: if $a_1 \neq 0$, $\phi_1 \neq 0$, $a_2 \neq 0$, $\phi_2 \neq 0$,
- or semi-trivial solution: if $a_1 = 0$, $\phi_1 = 0$, $a_2 \neq 0$, $\phi_2 \neq 0$.

Nontrivial amplitudes and phases have been found numerically by applying Newton–Raphson algorithm to the nonlinear algebraic equations (41)–(44) (putting $\dot{a}_1 = 0$, $\dot{\phi}_1 = 0$, $\dot{a}_2 = 0$, $\dot{\phi}_2 = 0$). Semi-trivial solutions have been found putting the first quasi-normal co-ordinate equal to zero $a_1 = 0, \phi_1 = 0$. Then, the semi-trivial solution for the amplitude of second quasi-normal coordinate and phase takes forms:

$$2\vartheta\dot{a}_2 = -\frac{1}{2}\tilde{\mu}\eta_1 a_2(1 - M\lambda_{22})\sin 2\phi_2 + a_2\vartheta\chi\left(-\tilde{\alpha}_2 + \frac{1}{4}a_2^2\tilde{\beta}_2\chi^2\right)M\lambda_{22}, \tag{47}$$

$$2\vartheta a_2\varepsilon\dot{\phi}_2 = a_2\left(p_2^2 - \vartheta^2\right) + \frac{3}{4}\varepsilon\tilde{\gamma}_1 a_2^3\psi_1^3 - \frac{1}{2}\varepsilon\tilde{\mu}\eta_1 a_2(1 - M\lambda_{22})\cos 2\phi_2. \tag{48}$$

In this case, in a steady state ($\dot{a}_2 = 0$, $\dot{\phi}_2 = 0$), after rearranging (47), (48) we get the characteristic equation

$$\begin{aligned}
&\varepsilon^2 a_2^4 \left(9\tilde{\gamma}_1^2 \psi_1^6 + \beta_2^2 \vartheta^2 \chi^6 M^2 \lambda_{22}^2\right) \\
&+8\varepsilon a_2^2 \left(-3\tilde{\gamma}_1 (p_2^2 - \vartheta^2)\psi_1^3 + \varepsilon \tilde{\alpha}_2 \tilde{\beta}_2 \vartheta^2 \chi^4 M^2 \lambda_{22}^2\right) \\
&-4\varepsilon^2 \tilde{\mu}^2 \eta_1^2 (1 - M\lambda_{22})^2 + 16\varepsilon^2 \tilde{\alpha}_2^2 \vartheta^2 \chi^2 M^2 \lambda_{22}^2 + \left(p_2^2 - \vartheta^2\right)^2 = 0,
\end{aligned} \tag{49}$$

which let us determine semi-trivial amplitudes. To find bifurcation points, trivial ($a_2 = 0$) into semi-trivial ($a_2 \neq 0$) solutions, we substitute $a_2 = 0$ in (49) and then we get

$$\vartheta_{1,2}^* = \sqrt{p_2^2 - \tilde{\alpha}_2^2 \chi^2 M^2 \lambda_{22}^2 \mp \sqrt{\Delta}}, \tag{50}$$

where

$$\Delta = \tilde{\alpha}_2^2 \chi^2 M^2 \lambda_{22}^2 \left(\tilde{\alpha}_2^2 \chi^2 M^2 \lambda_{22}^2 - 4p_2^2\right) + \tilde{\mu}^2 \eta_1^2 (1 - M\lambda_{22})^2 . \tag{51}$$

Two bifurcation points can appear if $\Delta > 0$ and

$$\mu > \frac{\alpha_2 \chi M \lambda_2 \sqrt{4p_2^2 - \alpha_2^2 \chi^2 M^2 \lambda_2^2}}{\eta_1 (1 - M\lambda_2)}. \tag{52}$$

For the weakly nonlinear system the parameter α_2 is small and then the bifurcation points appear if

$$\frac{\mu}{\alpha_2} > \sim 2 \frac{p_2 \chi M \lambda_2}{\eta_1 (1 - M\lambda_2)}. \tag{53}$$

This inequality is in accordance with results obtained for one degree of freedom system [8,9].

3.2. Combination Resonance

Besides the principal parametric resonances, the combination resonance near $\vartheta \approx (p_1 + p_2)/2$ is also interesting for the considered model. Taking into account the internal resonance condition $p_2 = 3p_1$, in the neighbourhood of combination resonance we can write $\vartheta^2 = ((p_1 + p_2)/2)^2 + \varepsilon\sigma_3$, and then we get

$$\vartheta^2 = 4p_1^2 + \varepsilon\sigma_3, \tag{54}$$

where σ_3 is detuning parameter near the combination resonance. In this case equations (7) and (8) take the form:

$$\ddot{Y}_1 + \frac{1}{4}\vartheta^2 Y_1 = \varepsilon \left\{ \frac{1}{4}\sigma_3 Y_1 + \tilde{F}_1(Y_1, Y_2, \dot{Y}_1, \dot{Y}_2, \tau) + M\lambda_{21} \tilde{F}_2(Y_1, Y_2, \dot{Y}_1, \dot{Y}_2, \tau) \right\}, \tag{55}$$

$$\ddot{Y}_2 + \frac{9}{4}\vartheta^2 Y_2 = \varepsilon \left\{ \frac{9}{4}\sigma_3 Y_2 + \tilde{F}_1(Y_1, Y_2, \dot{Y}_1, \dot{Y}_2, \tau) + M\lambda_{22} \tilde{F}_2(Y_1, Y_2, \dot{Y}_1, \dot{Y}_2, \tau) \right\}. \tag{56}$$

Functions $\tilde{F}_1(Y_1, Y_2, \dot{Y}_1, \dot{Y}_2, \tau)$ and $\tilde{F}_2(Y_1, Y_2, \dot{Y}_1, \dot{Y}_2, \tau)$ are defined in Section 2. Substituting (13) and (14) in (55) and (56) we obtain at the different perturbation orders:

ε^0

$$D_0^2 Y_{10} + \frac{1}{4}\vartheta^2 Y_{10} = 0, \tag{57}$$

$$D_0^2 Y_{20} + \frac{9}{4}\vartheta^2 Y_{20} = 0, \tag{58}$$

ε^1

$$D_0^2 Y_{11} + \frac{1}{4}\vartheta^2 Y_{11} = \frac{1}{4}\sigma_3 Y_{10} - 2D_0 D_1 Y_{10} + \tilde{F}_{10} + M\lambda_{21}\tilde{F}_{20}, \tag{59}$$

$$D_0^2 Y_{21} + \frac{9}{4}\vartheta^2 Y_{21} = \frac{9}{4}\sigma_3 Y_{20} - 2D_0 D_1 Y_{20} + \tilde{F}_{10} + M\lambda_{22}\tilde{F}_{20}, \tag{60}$$

Around the combination resonance the solutions at the zero order read

$$Y_{10}(T_0, T_1, T_2) = A_{11}(T_1, T_2)\exp\left(\frac{1}{2}i\vartheta T_0\right) + \bar{A}_{11}(T_1, T_2)\exp\left(-\frac{1}{2}i\vartheta T_0\right), \tag{61}$$

$$Y_{20}(T_0, T_1, T_2) = A_{21}(T_1, T_2)\exp\left(\frac{3}{2}i\vartheta T_0\right) + \bar{A}_{21}(T_1, T_2)\exp\left(-\frac{3}{2}i\vartheta T_0\right), \tag{62}$$

After substituting equations (61) and (62) into (59), (60) and eliminating the secular producing terms we get the modulation equations:

$$\begin{aligned} 2\vartheta\dot{a}_1 = {} & \frac{3}{2}\tilde{\gamma}_1 a_1^2 a_2 \psi_1 \psi_2^2 \sin(3\phi_1 - \phi_2) - \mu\eta_1 a_2 (1 - M\lambda_{21}) \sin(\phi_1 + \phi_2) \\ & + \left[-\tilde{F}_{d21} + \tilde{F}_{d22}\cos(3\phi_1 - \phi_2)\right] M\lambda_{21}, \end{aligned} \tag{63}$$

$$\begin{aligned} 2\varepsilon\vartheta a_1\dot{\phi}_1 = {} & \frac{1}{2}a_1\left(4p_1^2 - \vartheta^2\right) - \frac{3}{2}\varepsilon\tilde{\gamma}_1\psi_2 a_1\left(2a_2^2\psi_1^2 + a_1^2\psi_2^2\right) \\ & - \varepsilon\tilde{\mu}\eta_1 a_2 (1 - M\lambda_{21})\cos(\phi_1 + \phi_2) \\ & + \frac{3}{2}\varepsilon\tilde{\gamma}_1 a_1^2 a_2 \psi_1 \psi_2^2 \cos(3\phi_1 - \phi_2) - \varepsilon\tilde{F}_{d22} M\lambda_{21}\sin(3\phi_1 - \phi_2), \end{aligned} \tag{64}$$

$$\begin{aligned} 2\vartheta\dot{a}_2 = {} & \frac{1}{6}\tilde{\gamma}_1 a_1^3 \psi_2^3 \sin(3\phi_1 - \phi_2) + \frac{1}{3}\tilde{\mu}\eta_2 a_1 (1 - M\lambda_{22})\sin(\phi_1 + \phi_2) \\ & + \left[\tilde{F}_{d23} - \tilde{F}_{d24}\cos(3\phi_1 - \phi_2)\right] M\lambda_{22}, \end{aligned} \tag{65}$$

$$\begin{aligned} 2\vartheta a_2\varepsilon\dot{\phi}_2 = {} & \frac{3}{2}a_2\left(4p_1^2 - \vartheta^2\right) + \frac{1}{2}\varepsilon\tilde{\gamma}_1\psi_1 a_2\left(2a_1^2\psi_2^2 + a_2^2\psi_1^2\right) \\ & + \frac{1}{3}\varepsilon\tilde{\mu}\eta_2 a_1 (1 - M\lambda_{22})\cos(\phi_1 + \phi_2) \\ & - \frac{1}{6}\varepsilon\tilde{\gamma}_1 a_1^3 \psi_2^3 \cos(3\phi_1 - \phi_2) - \tilde{F}_{d24}\sin(3\phi_1 - \phi_2) M\lambda_{22}. \end{aligned} \tag{66}$$

Approximate solutions under the combination resonance condition are determined as

$$Y_1 = a_1 \cos\left(\frac{1}{2}\vartheta\tau + \phi_1\right) + \varepsilon(\ldots), \tag{67}$$

$$Y_2 = a_2 \cos\left(\frac{3}{2}\vartheta\tau + \phi_2\right) + \varepsilon(\ldots), \tag{68}$$

Complete forms of the above solutions are included in equations (A5) and (A6).

3.3. Stability Analysis

The stability of the approximate solution has been determined by analysing the modulation equations around the first principal (equations (25)–(28)), the second principal (equations (41)–(44)) and the combination resonance (equations (63)–(66)) conditions. All the modulation equations can be expressed in compact form as a set of the first ODE's

$$\begin{aligned}
\dot{a}_1 &= f_1(a_1, \phi_1, a_2, \phi_2), \\
\dot{\phi}_1 &= f_2(a_1, \phi_1, a_2, \phi_2), \\
\dot{a}_2 &= f_3(a_1, \phi_1, a_2, \phi_2), \\
\dot{\phi}_2 &= f_4(a_1, \phi_1, a_2, \phi_2),
\end{aligned} \tag{69}$$

In a steady state

$$\begin{aligned}
f_1(a_1, \phi_1, a_2, \phi_2) &= 0, \qquad f_2(a_1, \phi_1, a_2, \phi_2) = 0, \\
f_3(a_1, \phi_1, a_2, \phi_2) &= 0, \qquad f_4(a_1, \phi_1, a_2, \phi_2) = 0.
\end{aligned}$$

Perturbing (69) by substituting

$$\tilde{a}_1 = a_1 + \delta_1, \quad \tilde{\phi}_1 = \phi_1 + \delta_2, \quad \tilde{a}_2 = a_2 + \delta_3, \quad \tilde{\phi}_2 = \phi_2 + \delta_4$$

and considering the steady-state solutions, we get a set of linear equations in variations

$$\begin{aligned}
\frac{\mathrm{d}\delta_1}{\mathrm{d}\tau} &= \left(\frac{\partial f_1}{\partial a_1}\right)_0 \delta_1 + \left(\frac{\partial f_1}{\partial \phi_1}\right)_0 \delta_2 + \left(\frac{\partial f_1}{\partial a_2}\right)_0 \delta_3 + \left(\frac{\partial f_1}{\partial \phi_2}\right)_0 \delta_4, \\
\frac{\mathrm{d}\delta_2}{\mathrm{d}\tau} &= \left(\frac{\partial f_2}{\partial a_1}\right)_0 \delta_1 + \left(\frac{\partial f_2}{\partial \phi_1}\right)_0 \delta_2 + \left(\frac{\partial f_2}{\partial a_2}\right)_0 \delta_3 + \left(\frac{\partial f_2}{\partial \phi_2}\right)_0 \delta_4, \\
\frac{\mathrm{d}\delta_3}{\mathrm{d}\tau} &= \left(\frac{\partial f_3}{\partial a_1}\right)_0 \delta_1 + \left(\frac{\partial f_3}{\partial \phi_1}\right)_0 \delta_2 + \left(\frac{\partial f_3}{\partial a_2}\right)_0 \delta_3 + \left(\frac{\partial f_3}{\partial \phi_2}\right)_0 \delta_4, \\
\frac{\mathrm{d}\delta_4}{\mathrm{d}\tau} &= \left(\frac{\partial f_4}{\partial a_1}\right)_0 \delta_1 + \left(\frac{\partial f_4}{\partial \phi_1}\right)_0 \delta_2 + \left(\frac{\partial f_4}{\partial a_2}\right)_0 \delta_3 + \left(\frac{\partial f_4}{\partial \phi_2}\right)_0 \delta_4.
\end{aligned} \tag{70}$$

Index '0' means a derivative at the steady state. Considering the solutions of equations (70) in the form:

$$\delta_1 = C_1 \mathrm{e}^{\rho\tau}, \quad \delta_2 = C_2 \mathrm{e}^{\rho\tau}, \quad \delta_3 = C_3 \mathrm{e}^{\rho\tau}, \quad \delta_4 = C_4 \mathrm{e}^{\rho\tau} \tag{71}$$

we get the characteristic equation

$$Det\begin{bmatrix} \left(\frac{\partial f_1}{\partial a_1}\right)_0 - \rho & \left(\frac{\partial f_1}{\partial \phi_1}\right)_0 & \left(\frac{\partial f_1}{\partial a_2}\right)_0 & \left(\frac{\partial f_1}{\partial \phi_1}\right)_0 \\ \left(\frac{\partial f_2}{\partial a_1}\right)_0 & \left(\frac{\partial f_2}{\partial \phi_1}\right)_0 - \rho & \left(\frac{\partial f_2}{\partial a_2}\right)_0 & \left(\frac{\partial f_2}{\partial \phi_1}\right)_0 \\ \left(\frac{\partial f_3}{\partial a_1}\right)_0 & \left(\frac{\partial f_3}{\partial \phi_1}\right)_0 & \left(\frac{\partial f_3}{\partial a_2}\right)_0 - \rho & \left(\frac{\partial f_3}{\partial \phi_1}\right)_0 \\ \left(\frac{\partial f_4}{\partial a_1}\right)_0 & \left(\frac{\partial f_4}{\partial \phi_1}\right)_0 & \left(\frac{\partial f_4}{\partial a_2}\right)_0 & \left(\frac{\partial f_4}{\partial \phi_1}\right)_0 - \rho \end{bmatrix} = 0. \tag{72}$$

Stability of the approximate solutions depends on the value of the roots of the characteristic equation. The solutions are stable if the real part of the eigenvalue ρ is negative.

4. Numerical Example

Parameters of the considered coupled oscillators has to satisfy the internal resonance condition $p_2/p_1 = 3$. The relationship between the parameters M and δ_{12} which satisfy this condition is found from equation (5):

$$M = \frac{(41 - 9\delta_{12}) \pm 10\sqrt{16 - 9\delta_{12}}}{9\delta_{12}}. \tag{73}$$

Note that parameter $\delta_1 = 1$. Function $M = f(\delta_{12})$ is plotted in Figure 2.
Exemplary calculations have been done for the following system parameters values:

$$\alpha_2 = 0.01, \quad \beta_2 = 0.05, \quad \gamma_1 = 0.1, \quad M = 0.615832, \quad \delta_1, = 1, \quad \delta_{12} = 1. \tag{74}$$

Parameters M and δ_{12} correspond to point A located in Figure 2. Natural frequencies and parameters used for the system coordinates transformation take the values:

$$p_1 = 0.511, \quad p_2 = 1.534, \quad \lambda_{21} = 2.823, \quad \lambda_{22} = -0.575, \quad \chi = 0.294,$$
$$\psi_1 = 0.831, \quad \psi_2 = -0.169, \quad \eta_1 = 1.125, \quad \eta_2 = 0.125.$$

Nontrivial solutions of equations (25)–(28) which describe the resonance curve around the first natural frequency are presented in Figure 3.

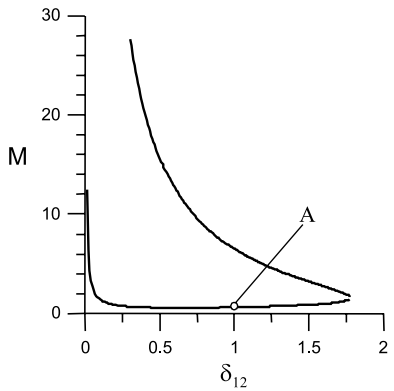

Figure 2. Condition of the internal resonance.

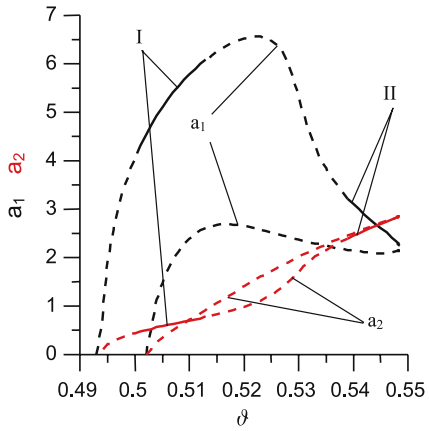

Figure 3. Resonance curves around the first natural frequency p_1.

Around the first natural frequency, nontrivial solutions for both amplitudes a_1 and a_2 are possible in the interval $\vartheta \in (0.493, 0.5485)$. However, stability analysis of solutions (25)–(28), presented in Section 3.2, proves that this region is divided in two stable parts. In the first region ($\vartheta \in (0.501, 0.513)$) the amplitude a_1 is much higher than amplitude a_2. It means that in the region I, of Figure 3, first vibration modes dominates while the second one is smaller but not negligible.

In the second part, region II in Figure 3, $\vartheta \in (0.539, 0.5485)$, the amplitudes of both modes are comparable. These two stable nontrivial intervals correspond to the synchronisation phenomenon. In both the stable regions I and II, the parametric excitation involves self-sustained oscillations. The response of the system is periodic and in the relevant Poincaré section two points are observed. But the synchronisation effect is broken down in the middle of the resonance area divided in two separate parts. This phenomenon does not take place for systems without internal resonance condition (e.g. Refs. [4, 5]). Dark regions on bifurcation diagrams in Figure 4 represent quasi-periodic motions, in which strong influence of self-excitation takes place. Solid line in these diagrams denotes synchronisation phenomenon. Theoretical results are in good agreement with bifurcation diagrams obtained numerically. However, numerical simulation gives a little wider areas.

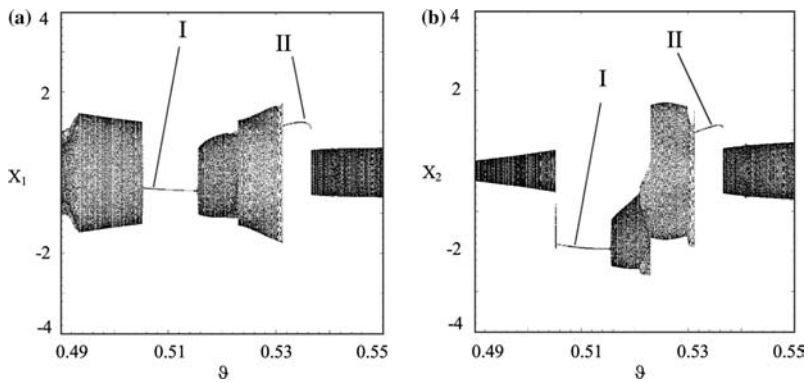

Figure 4. Bifurcation diagrams, generalised coordinates X_1 (a) and X_2 (b) versus ϑ parameter around the first natural frequency p_1.

The synchronisation effect is clearly visible for exemplary time histories obtained from direct numerical simulation of the original equations (3) and (4) and plotted in Figure 5. The motion in generalised coordinates X_1 and X_2 after transformation to quasi-normal coordinates Y_1, Y_2 is decoupled in two modes having frequency ϑ (Figure 5c) and frequency 3ϑ (Figure 5d). Outside the resonance the motion transits from periodic to quasi-periodic with modulated amplitude. Quasi-periodic motion is presented in Figure 6, where influence of self-excitation is clearly visible for both quasi-normal coordinates (Figure 6 c,d).

Around the second natural frequency p_2, apart from trivial (equal to zero) solution, two types of coexisting solutions are possible: semi-trivial solution if: $a_1 = 0$, $\phi_1 = 0$, $a_2 \neq 0$, $\phi_2 \neq 0$, or nontrivial solution if: $a_1 \neq 0$, $\phi_1 \neq 0$, $a_2 \neq 0$, $\phi_2 \neq 0$. The

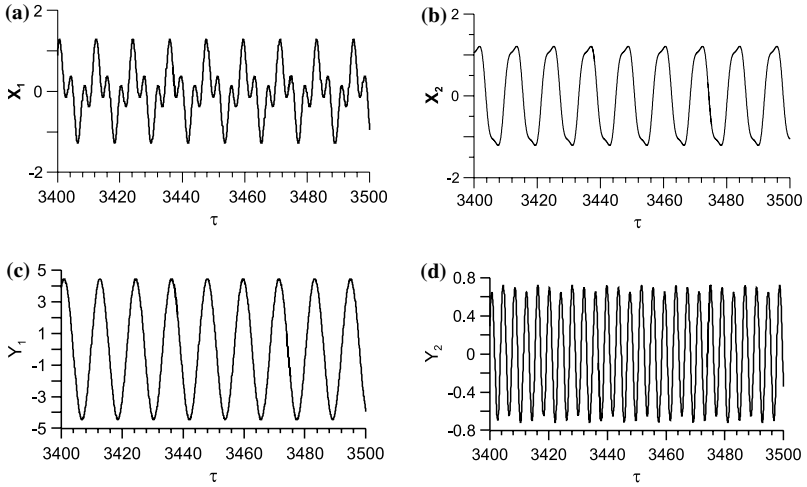

Figure 5. Time histories in generalised X_1 (a), X_2 (b) and quasi-normal coordinates Y_1 (c), Y_2 (d); $\vartheta = 0.534$.

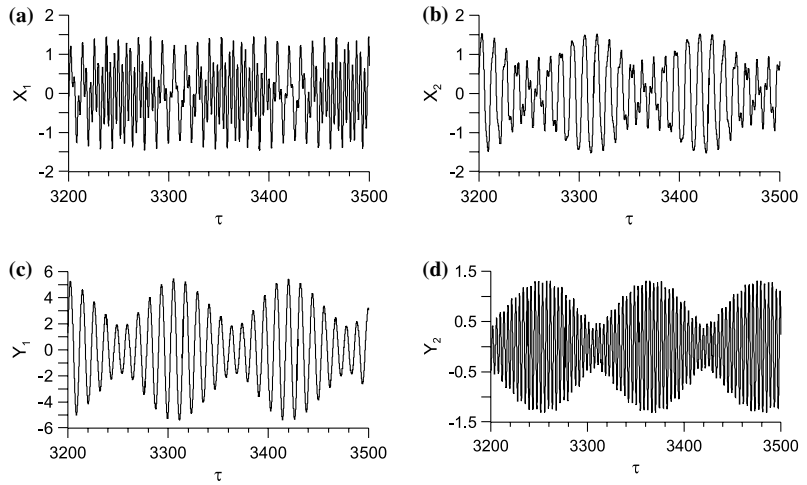

Figure 6. Time histories in generalised X_1 (a), X_2 (b) and quasi-normal coordinates Y_1 (c), Y_2 (d); $\vartheta = 0.52$.

perturbational frequency-amplitude response curves relevant to the semi-trivial and non-trivial solutions are presented in Figure 7.

Semi-trivial solutions attaining large amplitudes are theoretically possible in a wide area ($\vartheta \in (1.5, 4.1)$). Nontrivial solutions occur in the area marked by a rectangle. The zoom of this area is presented in Figure 8. The behaviour of the system in this resonance condition is qualitatively different respect on what seen around the first natural frequency. Around frequency p_2, the break of the synchronisation phenomenon does not take place. Nontrivial solutions, which represent the synchronised vibrations are confirmed by numerical simulation on bifurcation diagrams in Figure 9. The numerical simulations shows that the frequency interval in which the synchronisation phenomenon arises is wider then the corresponding analytical one. Semi-trivial solutions could have been confirmed numerically by analysis in details of their basins of attractions. The system tends to this kind of solution in a very long time, and only for chosen initial conditions. It has not been got by using classical bifurcation diagrams. Moreover, the pure periodic motion corresponding to the second mode has not been confirmed by numerical simulations. An exemplary periodic motion, corresponding to the semi-trivial solution is marked as *ST* on Poincaré section in Figure 10 while the quasi-periodic motion is represented by the closed loop

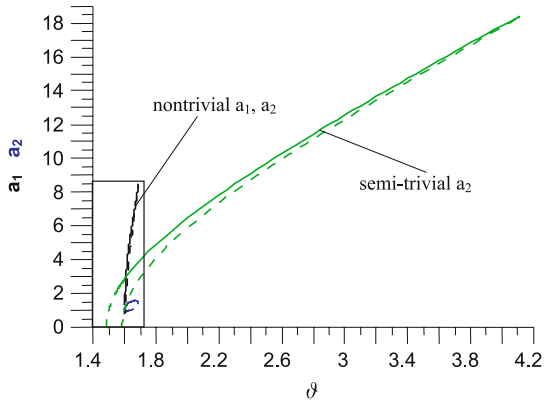

Figure 7. Amplitudes of semi-trivial and nontrivial solutions around the second natural frequency p_2.

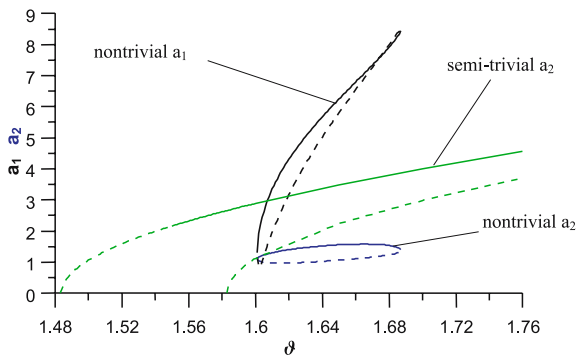

Figure 8. Amplitudes of nontrivial solutions around the second natural frequency, zoom of the area marked in Figure 7.

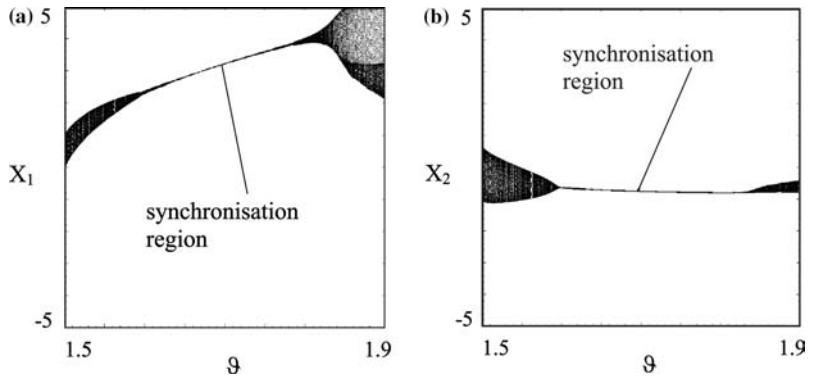

Figure 9. Bifurcation diagrams of generalised coordinates X_1 (a) and X_2 (b) versus ϑ parameter around the second natural frequency p_2.

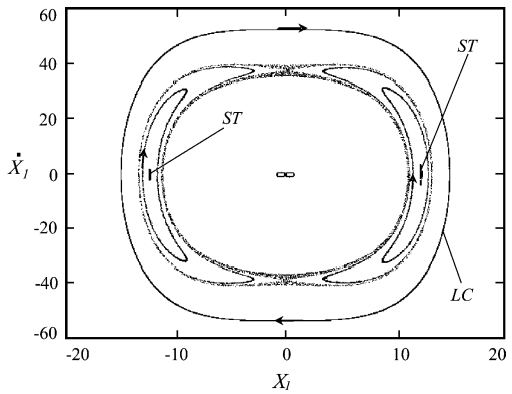

Figure 10. Poincaré section for $\vartheta = 3.6$.

LC. However, this motion is not represented only by one quasi-normal coordinate Y_2, what is clearly visible in time histories in Figure 11 a,b.

Combination resonance presented in Figure 12 consists of two separate pairs of curves. The synchronisation area is divided on two parts (I and II), similar to resonance around the frequency p_1. The synchronisation phenomenon, (solid line in Figure 13 is destroyed and quasi-periodic motion, inside the resonance, occurs (dark area in Figure 13). Outside this resonance, the system vibrates quasi-periodically (dark areas out of synchronisation in Figure 13). Apart from determined solutions, an additional quasi-periodic motion can appear in the system depending on initial conditions. Nevertheless, they are not found analytically by the proposed approach. Obtained analytically periodic motions in Figure 12 are in good agreement with the numerical simulation in Figure 13.

5. Transition to Chaotic Motion

Analysis of the parametric and self-excited systems published in former papers (e.g. Refs. [10, 12]), reveals that increase of parametric excitation causes important quantitative changes in the system dynamics. Exemplary bifurcation diagram versus parametric excitation amplitude μ is presented in Figure 14a. Numerical simulations have been done for the case defined by equation (74) and assuming the excitation frequency constant ($\vartheta = 1.0$). Bifurcation diagrams have been plotted for several initial conditions. Solid line in

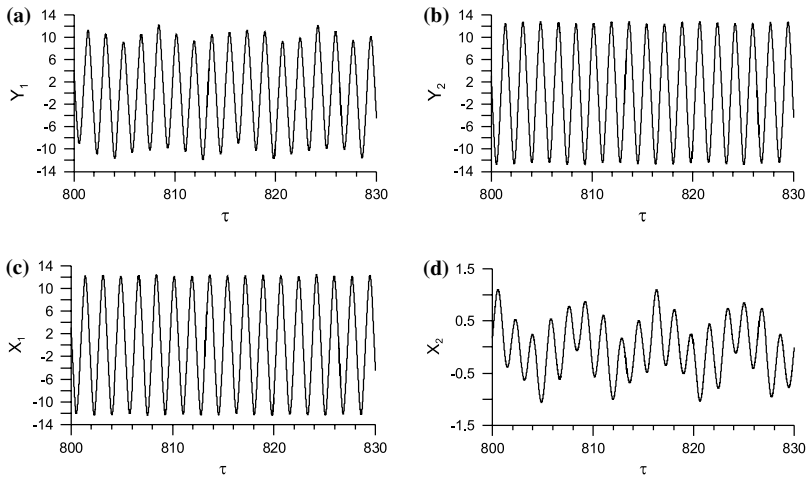

Figure 11. Time histories in quasi-normal coordinates Y_1 (a), Y_2 (b) and generalised X_1 (c), X_2 (d); $\vartheta = 3.6$.

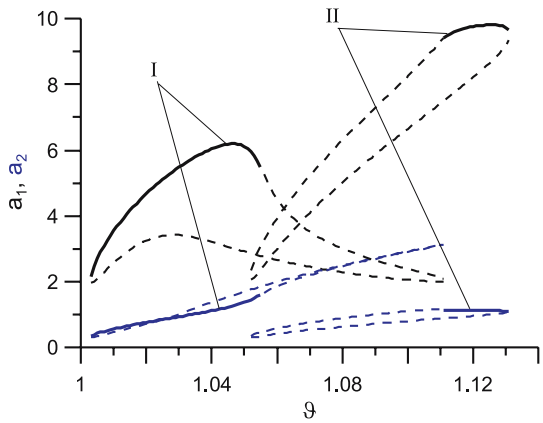

Figure 12. Vibration amplitudes around the combination resonance $(p_1 + p_2)/2$.

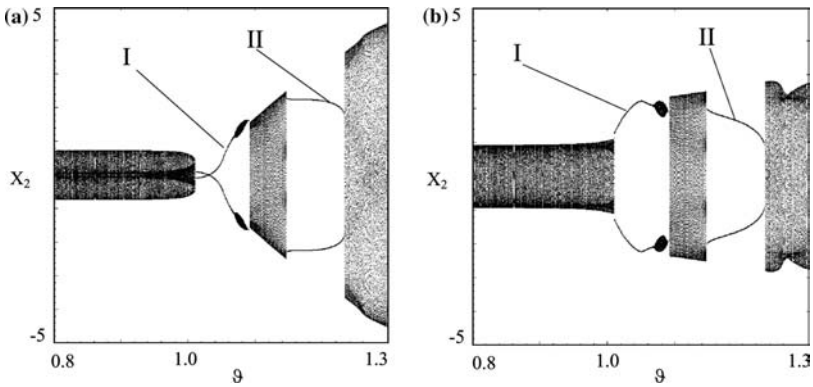

Figure 13. Bifurcation diagrams of generalised coordinates X_1 (a) and X_2 (b) versus ϑ parameter around the combination resonance.

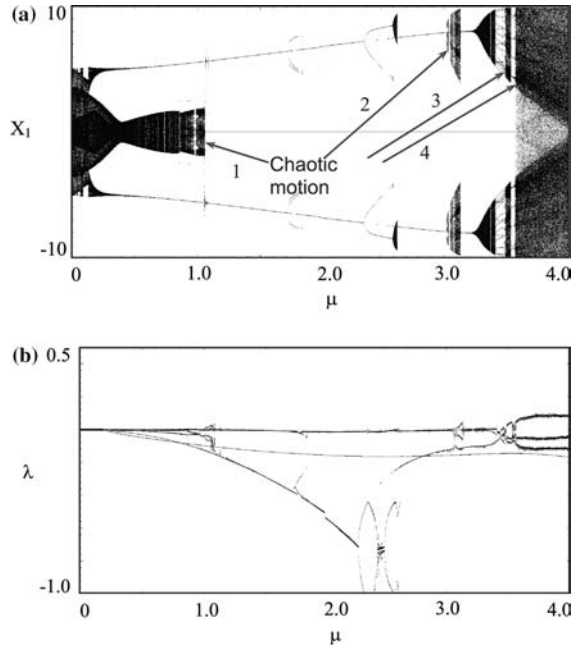

Figure 14. Bifurcation diagram (a) and Lyapunov's exponents (b) versus parametric excitation μ under internal resonance condition, $M = 0.615832$.

the Figure 14 a, corresponds to synchronised periodic vibrations while dark area to quasi-periodic or chaotic motion. The Lyapunov's exponent diagram in Figure 14b, reveals a chaotic response. The first chaotic motion (No.1) appears after a cascade of period doubling bifurcations near the parametric excitation $\vartheta \approx 1.0$. Then, after a boundary crisis the system transits to periodic motion. Different chaotic motion occur in areas No.2 $\vartheta \in (3.05;\ 3.15)$, No.3 $\vartheta \in (3.50;\ 3.53)$ and No. 4 $\vartheta \in (3.56;\ 4)$. In all the pointed regions the maximal Lyapunov's exponent is positive confirming the chaoticity of the motion.

Similar simulation has been done providing the system does not satisfy the internal resonance condition, parameter $M = 0.5$. This assumption means that point A on the curve in Figure 2 is a little shifted down from its original position $M = 0.615832$. The bifurcation diagram without internal resonance condition is presented in Figure 15. A smaller tendency in transition to chaos is observed in this case. Chaotic region No.1 is almost invisible in this case and regions No. 2, 3 have

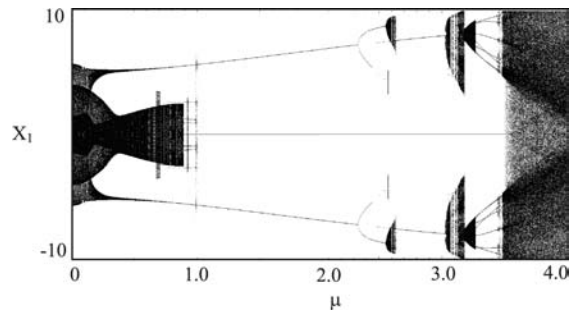

Figure 15. Bifurcation diagram versus parametric excitation μ without internal resonance condition, $M = 0.5$.

subintervals with periodic windows. Comparing Figures 14 and 15 we can conclude that internal resonance makes easier the transition of the system to chaos.

6. Conclusions

The analysis carried out in this paper, shows that under the internal resonance condition $p_2/p_1 = 3$, and around of the combination resonance $(p_1 + p_2)/2$ the synchronisation phenomenon in the neighbourhood of the principal parametric resonances' is possible. However, near the subharmonic and the combination resonance different behaviours are found in the case of presence or absence of the internal resonance condition. The synchronisation phenomenon appears in two separate intervals and the synchronised vibrations includes ϑ and 3ϑ components in both quasi-normal modes. Outside the resonance region, the motion besides ϑ and 3ϑ components, includes an additional incommensurable self-excited frequency and becomes quasi-periodic. Analytical results are in agreement with numerical simulations nevertheless showing synchronisation regions of wider area and shifted towards higher frequencies. Around the second natural frequency the synchronisation effect is observed only for nontrivial solutions and the relevant zone is not divided into sub-intervals. Near the second principal resonance, the semi-trivial solution is possible as well but the numerical simulation does not confirm existence of pure periodic semi-trivial motion.

The chaotic motion is possible under internal resonance condition for large values of the parametric excitation amplitude μ. The system under internal resonance condition has higher tendency in transition to chaotic motions compared to the case corresponding to the absence of such internal resonance condition. The results presented in this paper reveal only some possible motion of the model, mainly near the synchronisation phenomenon. The numerical simulation shows additional possible quasi-periodic solutions, which are not found analytically in this paper.

Appendix A

Approximate solutions around the first principal parametric resonance.

$$
\begin{aligned}
Y_1 = {} & a_1 \cos(\vartheta\tau + \phi_1) + \frac{1}{16\vartheta^2}\varepsilon\tilde{\mu}(1 - M\lambda_{21})\left[a_1\eta_2 \cos(3\vartheta\tau + \phi_1)\right. \\
& \left. - \frac{1}{3}a_2\eta_1 \cos(5\vartheta\tau + \phi_2)\right] + \frac{1}{32\vartheta^2}\varepsilon\tilde{\gamma}_1\left[-a_1^3\psi_2^3 \cos(3\vartheta\tau + 3\phi_1)\right. \\
& + 3a_2\psi_1\left(a_2^2\psi_1^2 + 2a_1^2\psi_2^2\right)\cos(3\vartheta\tau + \phi_2) + a_1^2a_2\psi_1\psi_2^2 \cos(5\vartheta\tau + 2\phi_1 + \phi_2) \\
& - a_1a_2^2\psi_1^2\psi_2 \cos(5\vartheta\tau - \phi_1 + 2\phi_2) - \frac{1}{2}a_1a_2^2\psi_1^2\psi_2 \cos(7\vartheta\tau + \phi_1 + 2\phi_2) \\
& \left. + \frac{1}{10}a_2^3\psi_1^3 \cos(9\vartheta\tau + 3\phi_2)\right] - \frac{3}{8\vartheta}M\lambda_{21}\varepsilon\tilde{\alpha}_2a_2\chi \sin(3\vartheta\tau + \phi_2) \\
& + \frac{1}{32\vartheta}M\lambda_{21}\varepsilon\tilde{\beta}_2\chi^3\left[-a_1^3 \sin(3\vartheta\tau + 3\phi_1) + 3a_2\left(2a_1^2 + a_2^2\right)\sin(3\vartheta\tau + \phi_2)\right. \\
& + \frac{5}{3}a_1^2a_2 \sin(5\vartheta\tau + 2\phi_1 + \phi_2) - \frac{5}{3}a_1a_2^2 \sin(5\vartheta\tau - \phi_1 + 2\phi_2) \\
& \left. - \frac{7}{6}a_1a_2^2 \sin(7\vartheta\tau + \phi_1 + 2\phi_2) + \frac{3}{10}a_2^3 \sin(9\vartheta\tau + 3\phi_2)\right], \qquad \text{(A1)}
\end{aligned}
$$

$$
\begin{aligned}
Y_2 = {} & a_2 \cos(3\vartheta\tau + \phi_2) + \frac{1}{16\vartheta^2}\varepsilon\tilde{\mu}\,(1 - M\lambda_{22})\,[-a_1\eta_2 \cos(\vartheta\tau - \phi_1) \\
& + a_2\eta_1 \cos(\vartheta\tau + \phi_2) - \frac{1}{2}a_2\eta_1 \cos(5\vartheta\tau + \phi_2)\Big] \\
& + \frac{3}{32\vartheta^2}\varepsilon\tilde{\gamma}_1\left[a_1\psi_2\left(a_1^2\psi_2^2 + 2a_2^2\psi_1^2\right)\cos(\vartheta\tau + \phi_1) - a_1^2 a_2\psi_1\psi_2^2 \cos(\vartheta\tau - 2\phi_1 + \phi_2)\right. \\
& + \frac{1}{2}a_1^2 a_2\psi_1\psi_2^2 \cos(5\vartheta\tau + 2\phi_1 + \phi_2) - \frac{1}{2}a_1 a_2^2\psi_1^2\psi_2 \cos(5\vartheta\tau - \phi_1 + 2\phi_2) \\
& \left. - \frac{1}{5}a_1 a_2^2\psi_1^2\psi_2 \cos(7\vartheta\tau + \phi_1 + 2\phi_2) + \frac{1}{27}a_2^3\psi_1^3 \cos(9\vartheta\tau + 3\phi_2)\right] \\
& - \frac{3}{8\vartheta}M\lambda_{22}\varepsilon\tilde{\alpha}_2 a_1\chi \sin(\vartheta\tau + \phi_1) + \frac{1}{32\vartheta}M\lambda_{22}\varepsilon\tilde{\beta}_2\chi^3\left[a_1\left(a_1^2 + 2a_2^2\right)\sin(\vartheta\tau + \phi_1)\right. \\
& - a_1^2 a_2 \sin(\vartheta\tau - 2\phi_1 + \phi_2) + \frac{5}{2}a_1^2 a_2 \sin(5\vartheta\tau + 2\phi_1 + \phi_2) \\
& - \frac{5}{2}a_1 a_2^2 \sin(5\vartheta\tau - \phi_1 + 2\phi_2) - \frac{7}{5}a_1 a_2^2 \sin(7\vartheta\tau + \phi_1 + 2\phi_2) \\
& \left. + \frac{1}{3}a_2^3 \sin(9\vartheta\tau + 3\phi_2)\right], \qquad \text{(A2)}
\end{aligned}
$$

Approximate solutions around the second principal parametric resonance.

$$
\begin{aligned}
Y_1 = {} & a_1 \cos\left(\frac{1}{3}\vartheta\tau + \phi_1\right) + \frac{3}{16\vartheta^2}\varepsilon\tilde{\mu}\,(1 - M\lambda_{21})\,[-3a_2\eta_1 \cos(\vartheta\tau - \phi_2) \\
& + a_1\eta_2 \cos\left(\frac{5}{3}\vartheta\tau - \phi_1\right) - \frac{1}{2}a_1\eta_2 \cos\left(\frac{7}{3}\vartheta\tau + \phi_1\right) - \frac{3}{10}a_2\eta_1 \cos(3\vartheta\tau + \phi_2)\Big] \\
& + \frac{9}{32\vartheta^2}\varepsilon\tilde{\gamma}_1\left[-a_1^3\psi_2^3 \cos(\vartheta\tau + 3\phi_1) + 3a_2\psi_1\left(a_2^2\psi_1^2 + 2a_1^2\psi_2^2\right)\cos(\vartheta\tau + \phi_2)\right. \\
& + a_1^2 a_2\psi_1\psi_2^2 \cos\left(\frac{5}{3}\vartheta\tau + 2\phi_1 + \phi_2\right) - a_1 a_2^2\psi_1^2\psi_2 \cos\left(\frac{5}{3}\vartheta\tau - \phi_1 + 2\phi_2\right) \\
& \left. - \frac{1}{2}a_1 a_2^2\psi_1^2\psi_2 \cos\left(\frac{7}{3}\vartheta\tau + \phi_1 + 2\phi_2\right) + \frac{1}{10}a_2^3\psi_1^3 \cos(3\vartheta\tau + 3\phi_2)\right] \\
& - \frac{9}{8\vartheta}M\lambda_{21}\varepsilon\tilde{\alpha}_2 a_2\chi \sin(\vartheta\tau + \phi_2) + \frac{3}{32\vartheta}M\lambda_{21}\varepsilon\tilde{\beta}_2\chi^3\left[-a_1^3 \sin(\vartheta\tau + 3\phi_1)\right. \\
& + 3a_2\left(2a_1^2 + a_2^2\right)\sin(3\vartheta\tau + \phi_2) + \frac{5}{3}a_1^2 a_2 \sin\left(\frac{5}{3}\vartheta\tau + 2\phi_1 + \phi_2\right) \\
& - \frac{5}{3}a_1 a_2^2 \sin\left(\frac{5}{3}\vartheta\tau - \phi_1 + 2\phi_2\right) - \frac{7}{6}a_1 a_2^2 \sin\left(\frac{7}{3}\vartheta\tau + \phi_1 + 2\phi_2\right) \\
& \left. + \frac{3}{10}a_2^3 \sin(3\vartheta\tau + 3\phi_2)\right], \qquad \text{(A3)}
\end{aligned}
$$

$$
\begin{aligned}
Y_2 = {} & a_2\cos(\vartheta\tau+\phi_2)+\frac{9}{16\vartheta^2}\varepsilon\tilde{\mu}(1-M\lambda_{22})\left[\frac{1}{2}a_1\eta_2\cos\left(\frac{5}{3}\vartheta\tau-\phi_1\right)\right.\\
& \left.+\frac{1}{5}a_1\eta_2\cos\left(\frac{7}{3}\vartheta\tau+\phi_1\right)-\frac{1}{9}a_2\eta_1\cos(3\vartheta\tau+\phi_2)\right]\\
& +\frac{27}{32\vartheta^2}\varepsilon\tilde{\gamma}_1\left[a_1\psi_2\left(a_1^2\psi_2^2+2a_2^2\psi_1^2\right)\cos\left(\frac{1}{3}\vartheta\tau+\phi_1\right)-a_1^2a_2\psi_1\psi_2^2\cos\left(\frac{1}{3}\vartheta\tau-2\phi_1+\phi_2\right)\right.\\
& +\frac{1}{2}a_1^2a_2\psi_1\psi_2^2\cos\left(\frac{5}{3}\vartheta\tau+2\phi_1+\phi_2\right)-\frac{1}{2}a_1a_2^2\psi_1^2\psi_2\cos\left(\frac{5}{3}\vartheta\tau-\phi_1+2\phi_2\right)\\
& \left.-\frac{1}{5}a_1a_2^2\psi_1^2\psi_2\cos\left(\frac{7}{3}\vartheta\tau+\phi_1+2\phi_2\right)+\frac{1}{27}a_2^3\psi_1^3\cos(3\vartheta\tau+3\phi_2)\right]\\
& -\frac{3}{8\vartheta}M\lambda_{22}\varepsilon\tilde{\alpha}_2a_2\chi\sin\left(\frac{1}{3}\vartheta\tau+\phi_1\right)+\frac{3}{32\vartheta}M\lambda_{22}\varepsilon\tilde{\beta}_2\chi^3\left[a_1\left(a_1^2+2a_2^2\right)\sin\left(\frac{1}{3}\vartheta\tau+\phi_1\right)\right.\\
& -a_1^2a_2\sin\left(\frac{1}{3}\vartheta\tau-2\phi_1+\phi_2\right)+\frac{5}{2}a_1^2a_2\sin\left(\frac{5}{3}\vartheta\tau+2\phi_1+\phi_2\right)\\
& -\frac{5}{2}a_1a_2^2\sin\left(\frac{5}{3}\vartheta\tau-\phi_1+2\phi_2\right)-\frac{7}{5}a_1a_2^2\sin\left(\frac{7}{3}\vartheta\tau+\phi_1+2\phi_2\right)\\
& \left.+\frac{1}{3}a_2^3\sin(3\vartheta\tau+3\phi_2)\right]. \qquad \text{(A4)}
\end{aligned}
$$

Approximate solutions around the combination resonance.

$$
\begin{aligned}
Y_1 = {} & a_1\cos\left(\frac{1}{2}\vartheta\tau+\phi_1\right)+\frac{1}{4\vartheta^2}\varepsilon\tilde{\mu}(1-M\lambda_{21})\left[a_1\eta_2\cos\left(\frac{3}{2}\vartheta\tau-\phi_1\right)\right.\\
& \left.+\frac{1}{3}a_1\eta_2\cos\left(\frac{5}{2}\vartheta\tau+\phi_1\right)-\frac{1}{6}a_2\eta_1\cos\left(\frac{7}{2}\vartheta\tau+\phi_2\right)\right]\\
& +\frac{1}{8\vartheta^2}\varepsilon\tilde{\gamma}_1\left[-a_1^3\psi_2^3\cos\left(\frac{3}{2}\vartheta\tau+3\phi_1\right)+3a_2\psi_1\left(a_2^2\psi_1^2+2a_1^2\psi_2^2\right)\cos\left(\frac{3}{2}\vartheta\tau+\phi_2\right)\right.\\
& +a_1^2a_2\psi_1\psi_2^2\cos\left(\frac{5}{2}\vartheta\tau+2\phi_1+\phi_2\right)-a_1a_2^2\psi_1^2\psi_2\cos(5\vartheta\tau-\phi_1+2\phi_2)\\
& \left.-\frac{1}{2}a_1a_2^2\psi_1^2\psi_2\cos\left(\frac{7}{2}\vartheta\tau+\phi_1+2\phi_2\right)+\frac{1}{10}a_2^3\psi_1^3\cos\left(\frac{9}{2}\vartheta\tau+3\phi_2\right)\right]\\
& -\frac{3}{4\vartheta}M\lambda_{21}\varepsilon\tilde{\alpha}_2a_2\chi\sin\left(\frac{3}{2}\vartheta\tau+\phi_2\right)+\frac{1}{16\vartheta}M\lambda_{21}\varepsilon\tilde{\beta}_2\chi^3\left[-a_1^3\sin\left(\frac{3}{2}\vartheta\tau+3\phi_1\right)\right.\\
& +3a_2\left(2a_1^2+a_2^2\right)\sin\left(\frac{3}{2}\vartheta\tau+\phi_2\right)+\frac{5}{3}a_1^2a_2\sin\left(\frac{5}{2}\vartheta\tau+2\phi_1+\phi_2\right)\\
& -\frac{5}{3}a_1a_2^2\sin\left(\frac{5}{2}\vartheta\tau-\phi_1+2\phi_2\right)-\frac{7}{6}a_1a_2^2\sin\left(\frac{7}{2}\vartheta\tau+\phi_1+2\phi_2\right)\\
& \left.+\frac{3}{10}a_2^3\sin\left(\frac{9}{2}\vartheta\tau+3\phi_2\right)\right], \qquad \text{(A5)}
\end{aligned}
$$

$$
\begin{aligned}
Y_2 = {} & a_2 \cos\left(\frac{3}{2}\vartheta\tau + \phi_2\right) \\
& + \frac{1}{4\vartheta^2}\varepsilon\tilde{\mu}\,(1 - M\lambda_{22})\left[a_2\eta_1 \cos\left(\frac{1}{2}\vartheta\tau - \phi_2\right) - \frac{1}{2}a_1\eta_2 \cos\left(\frac{5}{2}\vartheta\tau + \phi_1\right)\right. \\
& \left. - \frac{1}{5}a_2\eta_1 \cos\left(\frac{7}{2}\vartheta\tau + \phi_2\right)\right] + \frac{3}{8\vartheta^2}\varepsilon\tilde{\gamma}_1\left[a_1\psi_2\left(a_1^2\psi_2^2 + 2a_2^2\psi_1^2\right)\cos\left(\frac{1}{2}\vartheta\tau + \phi_1\right)\right. \\
& - a_1^2 a_2\psi_1\psi_2^2 \cos\left(\frac{1}{2}\vartheta\tau - 2\phi_1 + \phi_2\right) + \frac{1}{2}a_1^2 a_2\psi_1\psi_2^2 \cos\left(\frac{5}{2}\vartheta\tau + 2\phi_1 + \phi_2\right) \\
& - \frac{1}{2}a_1 a_2^2\psi_1^2\psi_2 \cos\left(\frac{5}{2}\vartheta\tau - \phi_1 + 2\phi_2\right) - \frac{1}{5}a_1 a_2^2\psi_1^2\psi_2 \cos\left(\frac{7}{2}\vartheta\tau + \phi_1 + 2\phi_2\right) \\
& \left. + \frac{1}{27}a_2^3\psi_1^3 \cos\left(\frac{9}{2}\vartheta\tau + 3\phi_2\right)\right] - \frac{1}{4\vartheta}M\lambda_{22}\varepsilon\tilde{\alpha}_2 a_1\chi \sin\left(\frac{1}{2}\vartheta\tau + \phi_1\right) \\
& + \frac{1}{16\vartheta}M\lambda_{22}\varepsilon\tilde{\beta}_2\chi^3\left[a_1\left(a_1^2 + 2a_2^2\right)\sin\left(\frac{1}{2}\vartheta\tau + \phi_1\right) - a_1^2 a_2 \sin\left(\frac{1}{2}\vartheta\tau - 2\phi_1 + \phi_2\right)\right. \\
& + \frac{5}{2}a_1^2 a_2 \sin\left(\frac{5}{2}\vartheta\tau + 2\phi_1 + \phi_2\right) - \frac{5}{2}a_1 a_2^2 \sin\left(\frac{5}{2}\vartheta\tau - \phi_1 + 2\phi_2\right) \\
& \left. - \frac{7}{5}a_1 a_2^2 \sin\left(\frac{7}{2}\vartheta\tau + \phi_1 + 2\phi_2\right) + \frac{1}{3}a_2^3 \sin\left(\frac{9}{2}\vartheta\tau + 3\phi_2\right)\right]. \qquad \text{(A6)}
\end{aligned}
$$

References

1. Awrejcewicz, J., *Bifurcation and Chaos. Theory and Application*, Springer Verlag, Berlin, 1994.
2. Kapitaniak, T. and Steeb, W.H., 'Transition to hyperchaos in coupled generalized Van der Pol's equations', *Phys. Lett. A* **152** (1991) 33–37.
3. Kononenko, W.O. and Kovalchuk, P., 'Influence of parametric excitation on self-excited system', *Prikladnaja Mechanika, Nauka, Glawnaja Redakcja Fiziko-Matiematiczeskoj Literatury* **7**(6) (1971) 3–10. (Moscow)
4. Tondl, A., *On the Interaction between Self-excited and Parametric Vibrations*, Monographs and Memoranda, No.25, National Research Institute for Machine Design, Prague, 1978.
5. Warminski, J., 'Synchronisation effects and chaos in van der Pol-Mathieu oscillator', *J. Theo. Appl. Mech.* **4**(39) (2001a) 861–884.
6. Szabelski, K. and Warminski, J., 'Vibrations of a non-linear self-excited system with two degrees of freedom under external and parametric excitation', *J. Nonlinear Dyn.* **14** (1997) 23–36.
7. Warminski, J., Litak, G. and Szabelski, K., 'Synchronisation and chaos in a parametrically and self-excited system with two degrees of freedom', *J. Nonlinear Dyn.* **22** (2000) 135–153.
8. Szabelski, K., and Warminski, J., 'The parametric self excited non-linear system vibrations analysis with the inertial excitation', *Int. J. Non-Linear Mech.* **30**(2) (1995a) 179–189.
9. Szabelski, K., and Warminski, J., 'The self-excited system vibrations with the parametric and external excitations', *J. Sound Vib.* **187**(4) (1995b) 595–607.
10. Warminski, J., *Regular and Chaotic Vibrations of Self- and Parametrically Excited Systems with Ideal and Non-Ideal Energy Sources (in Polish),* Lublin University of Technology Publishers, Lublin, Poland, 2001b.
11. Warminski, J., 'Influence of external force on the parametric and self-excited system', *J. Tech. Phys.* **42** (2001a) 349–366.
12. Warminski, J., 'Regular, chaotic and hyperchaotic vibrations of nonlinear systems with self, parametric and external excitations', *Sci. J. FACTA UNIVERSITATIS* **3**(14) (2003a) 891–905.
13. Warminski, J., Balthazar, J.M., and Brasil, R.M.L.R.F., 'Vibrations of non-ideal parametrically and self-excited model', *J. Sound Vib.* **245**(2) (2001) 363–374.

14. Warminski, J., 'Complexity and chaos of parametrically and self-excited system with non-ideal energy source', In Matthew P.C. (ed.), *Modern Practice in Stress and Vibration Analysis*, pp. 363–370 ttp Trans Tech Publications, Materials Science Forum, Switzerland, Germany, UK, USA, 2003b.
15. Bajkowski, J., and Szemplinska–Stupnicka, W., 'Internal resonances effects – simulation versus analytical methods results', *J. Sound Vib.* **104**(2) (1986) 259–275.
16. Bajkowski, J., *Internal Resonaces in Nonlinear Vibrating Systems, Part I (in Polish)*, Institute of Fundamental Technological Research, Polish Academy of Sciences, IPPT PAN, No.15, Warsaw, 1984.
17. Warminski, J., Litak, G., Cartmell, M.P., Khanin, R., and Wiercigroch, M., 'Approximate analytical solutions to the nonlinear primary metal cutting process', *J. Sound Vib.* **259**(4) (2003) 917–933.
18. Ishida, Y., and Inoue, T., 'Nonstationary oscillations of a nonlinear rotor during acceleration through the majar critical speed — Influence of internal resonance', *JSME Int. J. Series C-Mech. Sys. Machine Elements Manufacturing* **41**(3) (1998) 599–607.
19. Rusinek, R., Szabelski, K. and Warminski, J., 'Influence of the workpiece profile on the self-excited vibrations in metal turning process', In Radons, G. and Neugebauer, R., (ed.), *Nonlinear Dynamics of Production Systems*, Wiley-VCH, 2004, pp. 153–167.
20. Schmidt G., Interaction of self-excited, forced and parametrically excited vibrations, *Applications of the Theory of Nonlinear Oscillations – The 9th International Conference on Non-Linear Oscillations*, Naukova Dumka, Kiev, 1984, pp. 310–315.
21. Luongo, A., Paolone, A., and Piccardo, G., 'Postcritical behavior of cables undergoing two simultaneos galloping modes', *MECCANICA Int. J. Italian Assoc. Theo. Appl. Mech.* **33**(3) (1998) 229–242.
22. Lacarbonara, W., Rega, G. and Nayfeh, A.H., 'Resonant nonlinear normal modes. Part I: Analytical treatment for one-dimensional structural systems', *Int. J. Non-Linear Mech.* **38** (2003) 851–872.
23. Lacarbonara, W. and Rega, G., 'Resonant nonlinear normal modes. Part II: Activation/orthogonality conditions for shallow structural systems', *Int. J. Non-Linear Mech.* **38** (2003) 873–887.
24. Cartmell, M.P., 'On the need for control of nonlinear oscillations in machine systems', *MECCANICA Int. J. Ital. Assoc. Theo. Appl. Mech.* **38**(2) (2003) 185–212.
25. Nayfeh, A.H., *Introduction to Perturbation Technique*, Wiley, New York, 1981.